3-1990

Electron-Transport and Cyclotron-Resonance in [211]-Oriented HgTe-CdTe Superlattices

C. A. Hoffman

J. R. Meyer

Robert Wagner
Worcester Polytechnic Institute, rwagner@wpi.edu

F. J. Bartoli

X. Chu

See next page for additional authors

Electron transport and cyclotron resonance in [211]-oriented HgTe–CdTe superlattices

C. A. Hoffman, J. R. Meyer, R. J. Wagner, and F. J. Bartoli
Naval Research Laboratory, Washington, D. C. 20375

X. Chu and J. P. Faurie
University of Illinois at Chicago, Chicago, Illinois 60680

L. R. Ram-Mohan and H. Xie
Worcester Polytechnic Institute, Worcester, Massachusetts 01609

(Received 4 October 1989, accepted 5 October 1989)

We discuss a magnetotransport and magneto-optical investigation of [211]-oriented HgTe–CdTe superlattices. Measurements were performed on seven *n*-type samples with well widths in the range 41–125 Å and energy gaps between 0 and 128 meV. Both magnetotransport and magneto-optical results give evidence for an additional electron species besides the superlattice electrons and holes usually observed. We show that although these have quasi-two-dimensional character, their mobilities are quite sensitive to the superlattice well thickness. These findings are interpreted in terms of band bending and charge transfer from the CdTe substrate into the superlattice. We also discuss the first theoretical calculations of the band structure for [211]-oriented HgTe–CdTe heterostructures.

I. INTRODUCTION

Magnetotransport and magneto-optics represent two of the most important methods for determining the band edge properties of a semiconductor. When the two are correlated, the combination is even more powerful since the information acquired is largely complementary. Here we report a magnetotransport and magneto-optical study of HgTe–CdTe superlattices grown along the [211] crystal axis. Besides providing accurate energy gaps as well as effective masses and mobilities for electrons in the superlattice, the measurements reveal the presence of an additional electron species that apparently does not reside throughout the bulk of the superlattice. This electron has tentatively been identified as a charge transfer carrier.

Charge transfer from the CdTe substrate into the superlattice can occur when the bands bend near the interface in order to equalize the Fermi levels of the two regions. For the case of a single heterojunction (HgTe–CdTe, HgTe–$Hg_{1-x}Cd_xTe$, or $Hg_{1-x}Cd_xTe$–CdTe), previous investigators have discussed the transfer of both electrons[1,2] and holes.[3] To our knowledge, only one previous study has discussed the more complex case of charge transfer into a Hg-based superlattice. For zero-gap $Hg_{1-x}Zn_xTe$–CdTe, Berroir *et al.*,[4] suggested that one of the observed magneto-optical transmission minima may be due to cyclotron resonance by charge transfer electrons. However, only a plausibility argument was given for this identification, without supporting evidence. In the present investigation, the additional carrier is observed not only in the magneto-optical spectra, but also in magnetotransport data over a broad range of temperatures (4.2–300 K) and in samples spanning a wide range of energy gaps (0–128 meV). We find that its properties are quite sensitive to the superlattice well thickness.

II. BAND STRUCTURE THEORY

To aid the interpretation of the experimental data, we have carried out the first band structure calculations for [211] HgTe–CdTe superlattices. This has been made possible through a generalization of the transfer-matrix algorithm[5] to the treatment of arbitrary growth directions. Rotation of the Hamiltonian has been performed by accounting for $J = 1/2$ and $J = 3/2$ angular momenta associated with the Γ_6, Γ_7, and Γ_8 bands in the 8×8 **k·p** model. The details of the rotation matrices have been specified by Weiler,[6] and the matrix multiplication is performed symbolically in order to obtain an efficient computer code. It has been verified that for the [100] orientation, the present **k·p** results agree to within ≈ 10 meV with HgTe–CdTe superlattice band structures previously calculated by the tight-binding method.[7] Strain has been included, the valence band offset is taken to be 350 meV,[8] and for [211] growth the barriers are assumed to contain 10% HgTe.

The orientational dependence of the superlattice band structure is due primarily to the warping and anisotropy of the heavy hole bands in bulk HgTe and CdTe. One finds that results for the [211] growth direction are intermediate between [100] and [111]. For HgTe–CdTe superlattices with energy gaps on the order of 100 meV, the [211] gap is as much as 25 meV smaller than the [100] gap, while E_g in [111] is approximately 40 meV smaller than in [100]. For semimetallic superlattices, the negative separation between the E1 and HH1 band edges at the zone center is roughly 10 meV larger for [211] than for [100], and 20 meV larger for [111] than [100]. In the following section, theoretical energy gaps for the [211] orientation will be compared directly with values determined experimentally.

We have not attempted to obtain quantitative results for the more difficult case in which the superlattice band struc-

 0734-2101/90/021200-06$01.00

ture is perturbed by band bending and charge transfer effects near the interface with the substrate. This problem must be treated through a self-consistent solution to Schrödinger's and Poisson's equations,[9,10] which are coupled since the spatial variation of the band bending is determined by the charge distribution of the transferred electrons. However, we will make some qualitative observations concerning the expected properties of charge transfer carriers.

Figure 1(a) schematically illustrates the bending of the bands near the interface between a CdTe layer and a semiconducting $Hg_{1-x}Cd_xTe$ layer ($x>0.16$), whose thicknesses are both large compared to the depletion widths (for simplicity, we show only the conduction band of each material). If we assume that there is a deep donor-like state in the CdTe, the bands must bend in the vicinity of the interface in order to match the Fermi energies in the two materials. As a consequence, electrons from the CdTe will transfer across the interface to form an accumulation layer in the $Hg_{1-x}Cd_xTe$. Assuming that the band bending is strong enough, bound states (labeled $E1_{CT}$ and $E2_{CT}$ in the figure) will form in the triangular-shaped well on the $Hg_{1-x}Cd_xTe$ side. Although these states are confined in the z-direction, they are free to move parallel to the interface (they are quasi-two-dimensional) and will contribute to in-plane transport.

In Fig. 1(b), we replace the thick $Hg_{1-x}Cd_xTe$ layer with a HgTe–CdTe superlattice. Far away from the interface, the electron states are nearly unperturbed superlattice levels ($E1_{SL}$, $E2_{SL}$, etc.). These states are quasi-three-dimensional since the barriers of the investigated samples are relatively thin and the wells are strongly coupled. However, near the interface, band bending causes the energy of the minibands to be misaligned, i.e., k_z is no longer a good quantum number. Mendez *et al.*[11] have discussed the effect of an electric field on electron and hole subbands in a superlattice. They point out that the minibands are transformed into a series of discrete levels, the Stark ladder. The spatial extent of the states is then determined by the strength of the electric field. In a weak field, the level splitting is small and the wave functions extend over many wells. However, for a strong field such as that shown in Fig. 1(b) in the region adjacent to the interface, the states are confined to a single well. These varying degrees of localization are indicated by the horizontal arrows in the figure. Like the nearly unperturbed states, the states in the charge transfer region should have in-plane effective masses and transport properties that are quite sensitive to the thickness of the superlattice wells. The experimental data strongly support this assertion. Nonetheless, superlattice charge transfer states also resemble the single interface states considered in Fig. 1(a), in that they are confined to the region near the interface and because there is significant accumulation (the Fermi level is far above the bottom of the band). Based on the experimentally determined charge transfer densities, the width of the band bending region is estimated to be on the order of 1000 Å (the bending is actually more gradual than that indicated schematically in the figure).

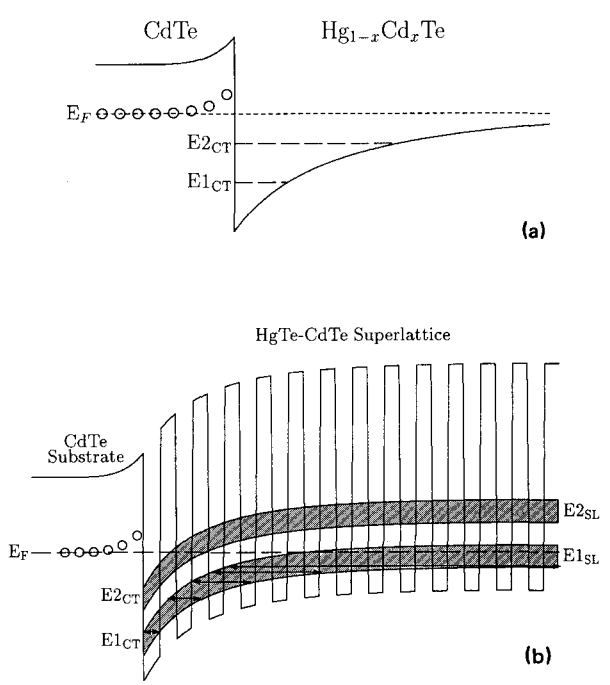

FIG. 1. (a) Schematic of conduction band bending and charge transfer for a CdTe–$Hg_{1-x}Cd_xTe$ interface. Deep CdTe donor and triangular-well energy levels are shown. (b) Schematic of conduction band bending and charge transfer for the interface between a CdTe substrate and a HgTe–CdTe superlattice. Charge transfer and nearly unperturbed superlattice energy bands are indicated. The shading indicates the miniband width, and the arrows indicate that the spatial extent of the states at a given position depends on the local electric field induced by the band bending.

III. MBE GROWTH AND MAGNETOTRANSPORT

Seven HgTe–$Hg_{0.10}Cd_{0.90}Te$ superlattices were grown by molecular-beam epitaxy (MBE). Deposition was directly onto a [211] CdTe substrate with no buffer layer (to our knowledge there has been only one previous investigation of [211]-orientation HgTe–CdTe superlattices).[12] The substrate temperature during growth was 195 °C. Of the seven superlattices, samples 1–4 have 150 periods while samples 5–7 have 100 periods. Table I lists well and barrier thicknesses (d_W and d_B) determined from x-ray satellite peaks.

van der Pauw Hall and conductivity measurements were performed on each of the seven samples as a function of magnetic field (0–70 kG) and temperature (4.2–300 K). Because multiple carrier species were almost always present, a mixed conduction analysis of the field-dependent data at a given temperature was performed in order to extract the densities and mobilities for the various carrier types. Table I

TABLE I. Sample characteristics.

No.	d_W (Å)	d_B (Å)	n_{SL}^0 (cm^{-3})	n_{CT} (cm^{-2})	E_g^{exp} (meV)	E_g^{theo} (meV)
1	125	41	4.7×10^{15}	≈0	$\leqslant3$	−43
2	107	42	5.1×10^{15}	9.5×10^{11}	$\leqslant3$	−41
3	92	42	2.5×10^{15}	2.2×10^{12}	$\leqslant6$	−31
4	74	36	2.2×10^{14}	1.0×10^{12}	$\leqslant8$	−13
5	75	36	1.0×10^{15}	2.3×10^{12}	$\leqslant14$	−14
6	45	37	9.6×10^{15}	2.7×10^{12}	88	71
7	41	36	5.9×10^{15}	1.9×10^{12}	128	90

gives low-temperature superlattice electron concentrations (n_{SL}^0) for each of the samples. These are seen to be less than $10^{16}\,cm^{-3}$ in all cases. With increasing temperature, n_{SL} was found to increase in a manner consistent with the thermal generation of intrinsic carriers. In previous studies of Hg-based superlattices, it has been demonstrated that analysis of the temperature dependence of n_i provides a valuable non-optical method for determining the zero-temperature energy gap (E_g^0).[13] Gaps determined in this manner for the present samples are listed in Table I. The two superlattices with the thinnest wells (6 and 7) were found to have relatively large E_g^0 of 88 and 128 meV, while samples 1–5 were all found to be semimetallic to within the experimental uncertainty,[14] i.e., $n_i \propto T^{3/2}$. Also shown in Table I are theoretical energy gaps calculated by the transfer-matrix method as discussed in Sec. II. Although the theory clearly reproduces the qualitative dependence of E_g^0 on d_W, the experimental gaps are underestimated by 18 and 38 meV in the two cases for which a comparison could be made. Uncertainty in the present x-ray determination of d_W is probably on the order of two monolayers ($\approx$7 Å). Decreasing d_W by less than that amount would bring theory and experiment into agreement for all samples. In a previous study of *p*-type HgTe–CdTe superlattices,[13] agreement was within 16 meV when comparison was made in the range of energy gaps for which the experimental method is expected to be most sensitive (0–80 meV).

For four different samples, Fig. 2 plots superlattice electron mobilities μ_{SL} as a function of temperature. It has been demonstrated previously[13] that low-temperature electron and hole mobilities in HgTe–CdTe superlattices tend to decrease with increasing energy gap, due to the approximate proportionality of the in-plane effective mass to E_g. This trend is clearly followed by the present data in that samples 6 and 7, which have significantly larger energy gaps, also have significantly lower μ_{SL}^0. On the other hand μ_{SL}^0 for these two

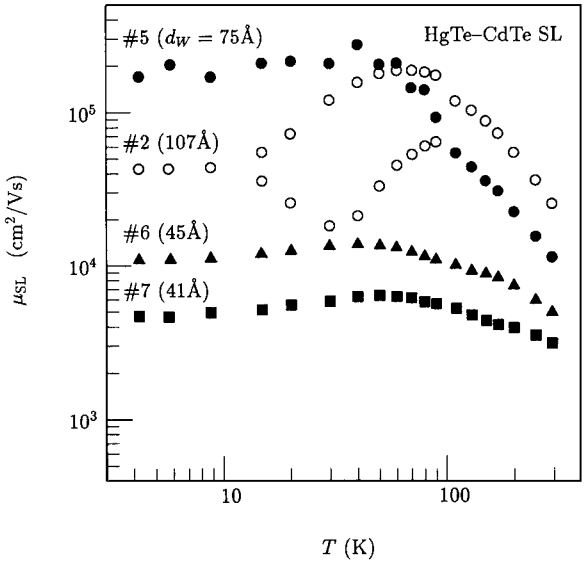

FIG. 2. Superlattice electron mobility vs. T for four samples. Sample numbers and well thicknesses are indicated.

samples are somewhat higher than those in samples with comparable E_g from the previous study.[13] In samples 4–7, which have well thicknesses of 75 Å or less, a single type of superlattice electron is observed. However, in samples 1–3 (92 Å $\leqslant d_W \leqslant$ 125 Å), the data indicate the presence of more than one species of high-mobility electron at temperatures between 15 and $\approx$ 100 K. For sample 2, the two mobilities are both given as open circles in Fig. 2 (the corresponding curves for samples 1 and 3 are quite similar). Theory in fact predicts that electrons with more than one mobility should be present simultaneously in semimetallic HgTe–CdTe superlattices. Band structure calculations[13] show that the electron effective mass is intrinsically broadened, i.e., electrons with a wide range of in-plane masses coexist within the superlattice (the two-electron experimental fit should be viewed as a simplified approximation to a continuous distribution of mobilities). While the effects of electron and hole mass-broadening have been observed previously in both magnetotransport[13,15,16] and magneto-optical studies,[17–19] in all previous work the broadening was observed down to 4.2 K rather than only above 15 K. Further study will be required to clarify the reason for the apparent suppression of mass broadening at the lowest temperatures in the present data.

The band structure calculation predicts that with increasing temperature, the E1-HH1 band separation at the center of the Brillouin zone increases. Thus, at 300 K all seven samples have positive energy gaps and μ_{SL} is found to decrease monotonically with decreasing well thickness (see Fig. 2). Again, this is due to the increase of the in-plane effective mass with increasing energy gap. This contrasts with the low-temperature regime, where E_g and the electron mass have their minima and μ_{SL}^0 peaks at an intermediate value of d_W. From Fig. 2 we see that sample 5 has the largest mobility at low T, but that the curves for samples 2 and 5 cross at higher T.

For all but one of the seven samples, the mixed-conduction analysis of the Hall and conductivity data indicate the presence of an additional electron species besides those which may be identified with the superlattice majority carrier. Whereas the density of superlattice electrons increases strongly with temperature as discussed in the previous paragraph, both the density and mobility of the additional electron are nearly independent of temperature over the entire range between 4.2 and 300 K. This is the behavior expected for a charge transfer carrier, since the high Fermi level in the region near the interface with the substrate causes the population to remain degenerate even at 300 K. The magneto-optical data discussed below also consistently indicates the presence of an additional carrier species, whose properties are consistent with the magnetotransport results. Tentatively identifying this carrier as being due to charge transfer, we list in Table I the density per unit area, n_{CT} for samples 2–7. Note that n_{CT} varies by less than a factor of three over the six samples, whereas n_{SL}^0 varies by more than a factor of 40.

Figure 3 plots temperature-dependent mobilities for the charge transfer carriers in the same four samples for which the superlattice mobilities are given in Fig. 2. Besides noting that $\mu_{CT} < \mu_{SL}$ in all cases, we find that there are clear quali-

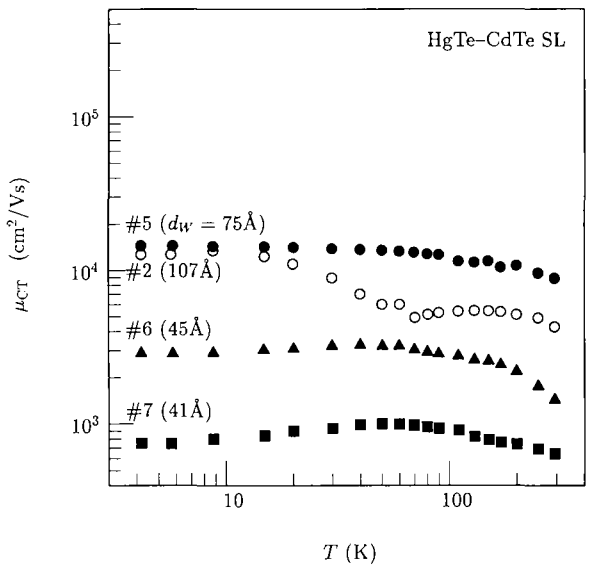

FIG. 3. Charge transfer electron mobility vs T for the same four superlattices as in Fig. 2. Sample numbers and well thicknesses are indicated.

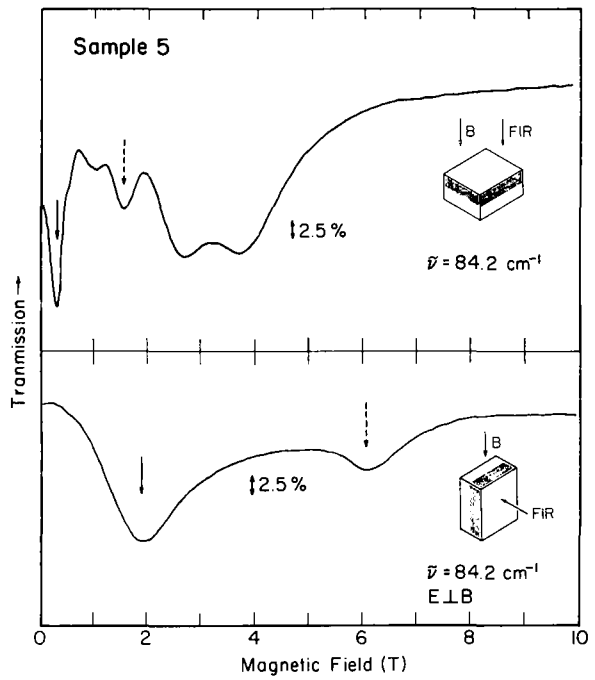

FIG. 4. Faraday (upper panel) and Voigt (lower panel) geometry magneto-optical spectra for sample 5 at 4.2 K. As the magnetic-field angle is rotated, the lines marked by the solid and dashed arrows in Faraday appear to evolve into the corresponding lines in Voigt.

tative trends as a function of well thickness. In particular, just as μ_{SL} decreases with decreasing k_W in samples with the thinnest wells, so does μ_{CT}. This probably occurs because the in-plane effective masses for both charge transfer and superlattice carriers depend strongly on d_W in the thin-well regime.

IV. MAGNETO-OPTICAL

Far infrared magnetotransmission measurements have been performed at 4.2 K on two of the samples, 5 and 6. The experimental approach is the same as that used previously to study p-type HgTe–CdTe superlattices.[17,18] Both samples displayed electron cyclotron resonance, along with other features at higher magnetic fields, which may be related to the charge transfer carriers.

Figure 4 shows typical spectra in both Faraday and Voigt geometries for sample 5. The arrows indicate that as the magnetic-field angle is rotated, the lines marked as solid or dashed in Faraday appear to evolve into the corresponding lines in Voigt. Both of these lines clearly exhibit quasi-three-dimensional (3D) behavior, since they exist in Voigt geometry under magnetic field conditions where the classical cyclotron orbit size is greater than the superlattice period. Similar anisotropic 3D behavior was observed previously for holes in a HgTe–CdTe superlattice.[17,18] In contrast, the absorption minima at 2.7 and 3.7 T in Faraday geometry were not observable in Voigt geometry. Although this suggests that they are quasi-2D, it should also be noted that as the magnetic field angle approached 90°, the increase of the resonance field with tilt angle was weaker and more complicated than that expected for a simple 2D dependence. If these lines are attributed to cyclotron resonance by charge transfer carriers, this may not be surprising since the states illustrated in Fig. 1(b) have a nonzero extent in the direction perpendicular to the interface with the substrate. At angles near 90° where the resonant magnetic fields are very large, the cyclotron orbit size may become smaller than the perpendicular extent of the wave functions and the resonance will have a mixture of 2D and 3D characteristics.

Using a recently developed theoretical formalism, which accounts for the strong dependence of the Landau level energies on growth-direction wave vector (k_z),[19,20] we have calculated the magnetic field dependence of the magneto-optical transmission in Faraday geometry. If the Fermi level at a given magnetic field is fixed by the condition that the total electron density must equal n_{SL}^0 determined from the magnetotransport results, the calculation yields an electron cyclotron resonance line quite similar to that marked by the solid arrow in Fig. 4. The calculated transmission minimum is found to be only $\approx$50% higher than that obtained experimentally. Furthermore, the half width of the experimental resonance indicates a mobility of 189 000, which agrees almost exactly with the low-temperature superlattice electron mobility μ_{SL} indicated in Fig. 2. Therefore, we can confidently identify the lowest-field line (solid arrow) as cyclotron resonance of the "unperturbed" superlattice electrons. The in-plane effective mass implied by the Faraday geometry data at 84.2 cm^{-1} is 0.0021 m_0, and comparison of the resonance fields in Faraday and Voigt geometries implies a mass anisotropy ratio m_z/m_x of 110. Such a large ratio is expected only if the superlattice is semimetallic, in which case the Γ-point conduction band is HH1.[4,13] For a semiconducting sample, the Γ-point conduction band is E1 and a much smaller anisotropy ratio is expected (see the results for sample 6 below).

The half widths of the two strong lines at 2.7 and 3.7 T

imply mobilities of 2.6×10^4 and 1.3×10^4 cm^2/V s, respectively. Note that these values bracket the mobility μ_{CT} shown in Fig. 3 for sample 5. Also, if one integrates the intensities to obtain the total number of carriers associated with these two lines, the ratio of the densities of low-mobility (2.7 and 3.7 T) to high-mobility (solid arrow) carriers is 18 to 1. This compares with a ratio of 22 to 1 obtained if n_{CT} from the magnetotransport is averaged over the superlattice thickness of 1.1 μm and divided by n_{SL}^0. This clearly supports a connection between the two high-field lines in the magnetotransmission spectrum and the lower-mobility electrons observed in the transport data.

The origin of the quasi-3D intermediate-field line marked by the dashed arrow remains unexplained (as well as a smaller feature at slightly lower fields in Faraday geometry). Calculations assuming no band bending yield that for low superlattice electron densities such as the experimentally-observed value of 10^{15} cm^{-3}, only states near $k_z = 0$, which have a very small in-plane mass, should be occupied. There are then no obvious features in the band structure that would lead to a resonance near 1.5 T. However, when the bands have bent by only $\approx$20 meV as the interface is approached (the total bending may be $>$100 meV), the local electron density is increased beyond $\approx3\times10^{16}$ cm^{-3} and the Fermi level increases to the point where the electron band is occupied at all k_z. Near $k_z = \pi/d$ the in-plane effective mass is much larger, leading to the possibility of cyclotron resonance at a field comparable to that indicated by the dashed arrow. States in the region approaching the interface where the electric field due to band bending is not yet very strong will have wave functions that extend over a number of superlattice wells. Transitions occurring in this region may have the quasi-3D character apparent for the line marked by the dashed arrows in Faraday and Voigt.

Magnetotransmission data for sample 6 indicate a distinct low-field resonance as well as some complicated structure between 2.3 and 7 T. The low-field line, which is clearly cyclotron resonance by the superlattice electrons, is seen in both Faraday and Voigt geometries. At 84.2 cm^{-1} the data yield $m_x = 0.011\ m_0$ and $m_z = 0.088\ m_0$. The band structure theory gives values of 0.013 and 0.080, which may be considered quite good agreement. Note that the electron mass is far less anisotropic in the semiconducting regime than it is for semimetallic superlattices. It seems likely that the structure at higher magnetic fields is related to the second electron observed in the magnetotransport. When the magnetic field is rotated from Faraday geometry, the high-field structure moves to higher magnetic fields until in Voigt it could not be observed at all up to fields of 12 T. This suggests a quasi-2D character, as expected for charge transfer carriers.

V. DISCUSSION

Our data show the presence of at least two species of electrons, one which is clearly the superlattice majority carrier and a second that we tentatively identify as a charge transfer electron. The magnetotransport data show that the superlattice electron density increases strongly with increasing temperature, and in semimetallic samples 1–5 its mobility also varies significantly with T. On the other hand, both the density and mobility for the second electron are nearly independent of T. The mobilities of both electrons decrease strongly with decreasing superlattice well thickness in semiconducting samples. The magneto-optical data also indicate the presence of at least two species of electrons. In the case of sample 5, positive correspondence can be made between the two electrons observed in magnetotransport and specific resonances in the magnetotransmission spectra. Whereas the superlattice electron is seen to have a 3D character, the second electron is more nearly quasi-2D (although the variation with field angle does not strictly follow a simple 2D dependence). Since the second carrier has 2D character with properties sensitive to the superlattice well thickness, the only possibilities would appear to be that it resides either on the front surface of the superlattice or at the interface between the superlattice and the substrate. Although Fig. 1(b) was drawn with the latter possibility in mind, both should have similar properties for a similar degree of band bending.

It should be noted that the higher-field magnetotransmission resonance observed by Berroir *et al.*[4] in two $Hg_{1-x}Zn_xTe$–CdTe superlattices displayed quasi-3D character, since it remained observable in Voigt geometry at magnetic fields of less than 3 T. In fact, it more closely resembles the unexplained intermediate-field resonance marked by the dashed arrows in our Fig. 4, whose connection to the charge transfer electrons requires further clarification.

Summarizing, we have performed a magnetotransport and magneto-optical investigation of HgTe–CdTe superlattices grown along the [211] crystal axis. Energy gaps determined from the temperature dependence of the intrinsic carrier density are compared to theoretical values obtained for the first time using band structure calculations for [211] HgTe–CdTe superlattices. Both the magnetotransport and the magneto-optical data indicate the presence of two different electron species. One is clearly the superlattice electron and the second has been tentatively identified as a charge transfer carrier. The measurements yield detailed properties for the charge transfer electron, including the strong dependence of its mobility on superlattice well thickness.

ACKNOWLEDGMENTS

One of us (L.R.R.) thanks K.-H. Yoo for valuable discussions and acknowledges the use of computer facilities at Worcester Polytechnic Institute. This research was partially supported by SDIO/IST and managed by the Naval Research Laboratory.

[1]Y. Guldner, G. S. Boebinger, J. P. Vieren, M. Voos, and J. P. Faurie, Phys. Rev. B **36**, 2958 (1987).
[2]R. J. Justice, D. G. Seiler, W. Zawadzki, R. J. Koestner, M. W. Goodwin, and M. A. Kinch, J. Vac. Sci. Technol. A **6**, 2779 (1988).
[3]J. P. Faurie, I. K. Sou, P. S. Wijewarnasuriya, S. Rafol, and K. C. Woo, Phys. Rev. B **34**, 6000 (1986).
[4]J. M. Berroir, Y. Guldner, J. P. Vieren, M. Voos, X. Chu, and J. P. Faurie, Phys. Rev. Lett. **62**, 2024 (1989).
[5]L. R. Ram-Mohan, K. H. Yoo, and R. L. Aggarwal, Phys. Rev. B **38**, 6151 (1988).
[6]M. H. Weiler, in *Semiconductors and Semimetals*, edited by R. K. Wil-

lardson and A. C. Beer (Academic, New York, 1981), Vol. 16, p. 119.
[7]J. R. Meyer, F. J. Bartoli, C. A. Hoffman, and J. N. Schulman, Phys. Rev. B **38**, 12457 (1988).
[8]J. R. Meyer, C. A. Hoffman, and F. J. Bartoli, Semicond. Sci. Technol. (in press).
[9]F. Stern and W. E. Howard, Phys. Rev. **163**, 816 (1967).
[10]T. Ando, A. B. Fowler, and F. Stern, Rev. Mod. Phys. **54**, 437 (1982).
[11]E. E. Mendez, F. Agullo–Rueda, and J. M. Hong, Phys. Rev. Lett. **60**, 2426 (1988).
[12]M. W. Goodwin, M. A. Kinch, R. J. Koestner, M. C. Chen, D. G. Seiler, and R. J. Justice, J. Vac. Sci. Technol. A **5**, 3110 (1987).
[13]C. A. Hoffman, J. R. Meyer, F. J. Bartoli, J. W. Han, J. W. Cook, Jr., J. F. Schetzina, and J. N. Schulman, Phys. Rev. B **39**, 5208 (1989).
[14]The uncertainty was somewhat greater than in past studies because of the high density of charge-transfer electrons. Both the high μ_n obtained from the magnetotransport results and the large mass anisotropy determined from the magneto-optical data suggest that Sample 5 is semimetallic.
[15]C. A. Hoffman, J. R. Meyer, F. J. Bartoli, J. W. Han, J. W. Cook, Jr., and J. F. Schetzina, Phys. Rev. B **40**, 3867 (1989).
[16]C. A. Hoffman, J. R. Meyer, F. J. Bartoli, J. W. Han, J. W. Cook, Jr., and J. F. Schetzina, Surf. Sci. (in press).
[17]J. M. Perez, R. J. Wagner, J. R. Meyer, J. W. Han, J. W. Cook, Jr., and J. F. Schetzina, Phys. Rev. Lett. **61**, 2261 (1988).
[18]R. J. Wagner, J. M. Perez, J. R. Meyer, J. W. Han, J. W. Cook, Jr., and J. F. Schetzina, J. Vac. Sci. Technol. A **7**, 411 (1989).
[19]J. R. Meyer, R. J. Wagner, F. J. Bartoli, C. A. Hoffman, and L. R. Ram-Mohan, Phys. Rev. B **40**, 1388 (1989).
[20]J. R. Meyer, R. J. Wagner, F. J. Bartoli, C. A. Hoffman, L. R. Ram-Mohan, M. Dobrowolska, T. Wojtowicz, and J. K. Furdyna (to be published).